

# Learning Navigation Skills for Legged Robots with Learned Robot Embeddings

Joanne Truong<sup>1,\*</sup>, Denis Yarats<sup>2</sup>, Tianyu Li<sup>2</sup>, Franziska Meier<sup>2</sup>, Sonia Chernova<sup>1,2</sup>, Dhruv Batra<sup>1,2</sup>, Akshara Rai<sup>2</sup>

**Abstract**—Navigation policies are commonly learned on idealized cylinder agents in simulation, without modelling complex dynamics, like contact dynamics, arising from the interaction between the robot and the environment. Such policies perform poorly when deployed on complex and dynamic robots, such as legged robots. In this work, we learn hierarchical navigation policies that account for the low-level dynamics of legged robots, such as maximum speed, slipping, and achieve good performance at navigating cluttered indoor environments. Once such a policy is learned on one legged robot, it does not directly generalize to a different robot due to dynamical differences, which increases the cost of learning such a policy on new robots. To overcome this challenge, we learn dynamics-aware navigation policies across multiple robots with robot-specific embeddings, which enable generalization to new unseen robots. We train our policies across three legged robots - 2 quadrupeds (A1, AlienGo) and a hexapod (Daisy). At test time, we study the performance of our learned policy on two new legged robots (Laikago, 4-legged Daisy) and show that our learned policy can sample-efficiently generalize to previously unseen robots.

## I. INTRODUCTION

Legged robots such as quadrupeds from Boston Dynamics [1], Unitree [5] and Ghost robotics [2] and Daisy hexapod from Hebi robotics [3] have emerged on the market as mature, robust, commercial robotic platforms. Legged robots are agile and can easily traverse uneven ground in homes like carpets and stairs, making them ideal for indoor navigation. At the same time, significant progress has been made in the field of learned indoor navigation using an egocentric camera input, without the use of maps [24], [27]. However, learned visual navigation literature typically considers idealized virtual cylindrical agents, and does not take the dynamics of the robot into account. While such policies can be successful on wheeled robots, legged robots have significantly different dynamics than an idealized agent or even other legged robots. These differences arise due to properties such as turning radius, motor strength, size and mass of the robot, etc. Fig. 1b shows an example where a PointGoal Navigation (PointNav) [6] policy that assumes an idealized agent is applied on the Daisy hexapod. While the policy plans to turn around an obstacle, the robot gets stuck, due to its larger size and turning radius, which were not accounted for by the PointNav policy. On the other hand, when the policy is

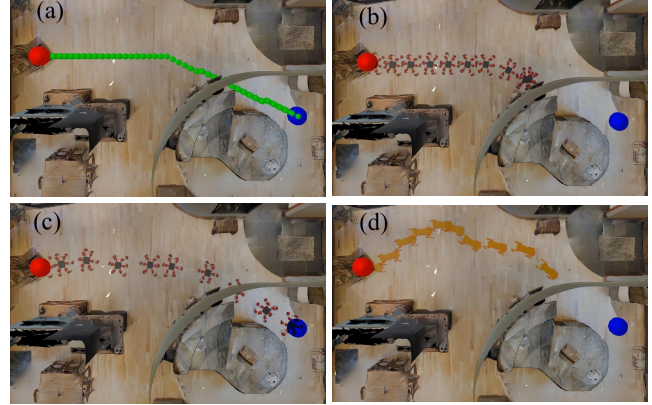


Fig. 1: Challenges of indoor navigation with legged robots. While an idealized spherical agent (a) can navigate to the goal with a PointNav policy, the same policy on Daisy (b) results in the robot getting stuck around an obstacle. A navigation policy trained on Daisy, with just egocentric images and no maps, can navigate to the goal successfully (c), but the same policy on the AlienGo quadruped (d) results in AlienGo drifting, and not reaching the goal in maximum allowed steps.

trained directly on Daisy (Fig. 1c), and thus is aware of the dynamics of the robot, the policy starts turning sooner to accommodate the large body and turning radius, leading to a successful navigation around the obstacle. Applying a policy that was learned on Daisy on another legged robot - the AlienGo quadruped (Fig. 1d) leads to the robot drifting away, and not reaching the goal in maximum allowed steps. This example highlights the importance of incorporating robot-specific dynamics when learning navigation policies for legged robots and the challenges of generalizing such learned policies to new robots. If navigation policies learned on one legged robot do not directly generalize to new systems, the experimental cost of learning navigation policies for legged robots can be prohibitively high, especially on hardware, reducing the overall scalability of such an approach. Learning navigation policies for complex legged robots, as well robustly transferring such learned policies to new robots are important challenges in the field of autonomous navigation.

In this work, we take a step towards learning visual navigation policies for legged robots, which use egocentric camera inputs and no maps, and generalize to new legged systems. We learn a navigation policy across three legged robots – two quadrupeds (A1, AlienGo) and one hexapod (Daisy), in three different simulated indoor home environments (Fig. 2), and test on previously unseen legged robots (Laikago, 4-

\*Work done while at FAIR

<sup>1</sup>Georgia Institute of Technology, {truong.j, dbatra, chernova}@gatech.edu

<sup>2</sup>Facebook AI Research {akshararai, fmeier, tianyu, denisy}@fb.com

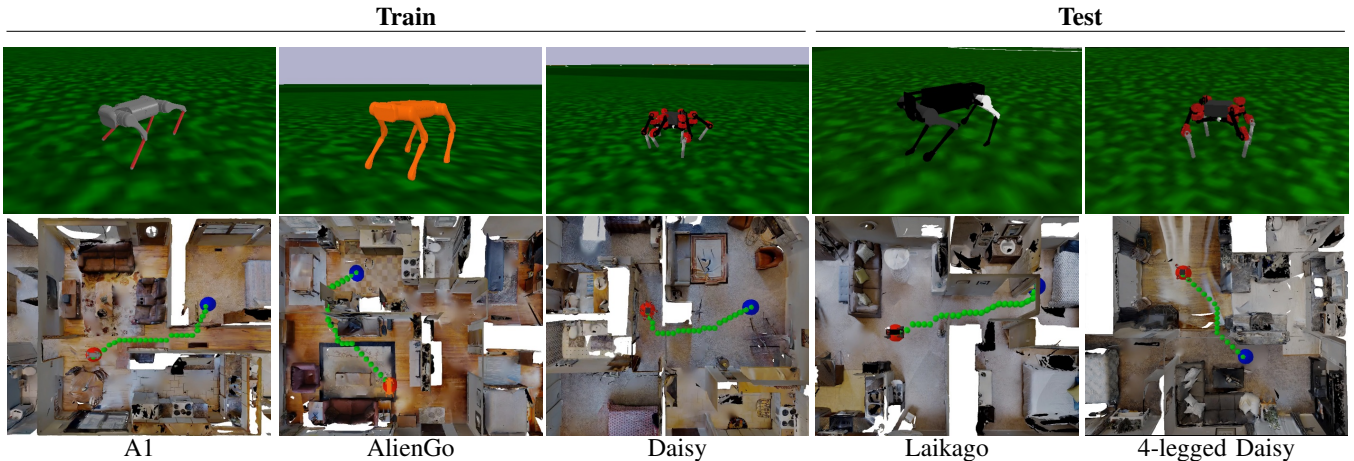


Fig. 2: Legged robots and environments used for training and testing. We train PointNav policies in cluttered environments on A1, AlienGo, and Daisy. At test-time, we study generalization to new legged robots – Laikago and 4-legged Daisy.

legged Daisy). We develop hierarchical navigation policies that divide the control of the robot into a high-level policy that reasons about the center of mass motion and a low-level policy that converts high-level (velocity) commands into desired footsteps. The high-level policy consists of two components: (1) a universal navigation policy (shared across multiple robots) and (2) a learned robot-specific embedding used to specialize the universal policy per robot. During training, we collect data from multiple robots in separate environments, contributing to a common replay buffer, improving sample-efficiency, and leading to a policy that is inherently robust to variations in robot dynamics. Once trained, this high-level policy can be used on new legged robots in unseen environments, by searching in the learned embedding space, keeping the learned policy fixed. To the best of our knowledge, this is the first work that (1) demonstrates learning navigation policies from visual input for legged robots; (2) learns navigation policies across multiple legged robots; and (3) generalizes learned policies to previously unseen legged robots.

The core contribution of this work is a sample-efficient approach for teaching legged robots to navigate unknown indoor environments. Instead of training a navigation policy per robot, we propose learning generalizable navigation policies that can be used on unseen robots in new environments. Such policies are inherently robust to dynamics and environment changes, as well as, open avenues for large-scale research in navigation with multiple legged robots. All our results are presented in the iGibson [29] photo-realistic simulation environment, with a Pybullet [9] physics engine, which has been used for sim-to-real transfer of learned navigation policies before [4]. Transferring our framework to real legged robots is an important next step.

## II. RELATED WORK

Navigation in unknown environments has been widely studied in robotics. We mention some closely related works. **Indoor Navigation:** Classical navigation approaches typically decompose the problem into mapping the environment, localizing in the map, and planning a path to the goal [11],

[25], [13]. However, such approaches are highly dependent on the quality of the map. Mappers that only utilize RGB-D images are prone to failure in texture-less regions, and may require the use of expensive LIDAR sensors [15]. Incomplete maps with errors often lead to poor performance when used by planners [7]. Additionally, the map building process can be time-consuming, and require user-designed semantics for more robust navigation [8]. Instead, we use a learned policy that learns to extract relevant information from depth images, using self-supervised and reinforcement learning.

Recent works have shown end-to-end learning-based approaches that utilize reinforcement learning to be robust in navigating previously unseen environments without explicit mapping (purely from egocentric RGB-D images and localization sensors) [24], [27]. However, these approaches have typically only been demonstrated on simple, cylindrical mobile base robots [17], and drones [23]. In contrast to these robots, legged robots have significantly more complex dynamics, arising from contacts and other interactions between the robot and the environment, and policies learned on one legged robot do not generalize to new legged robots directly. In this work, we propose to learn navigation policies for legged robots that are capable of generalizing to new robots.

**Context-aware transfer learning:** To adapt to new settings such as sim-to-real transfer, or adapting to new tasks, several works propose a context-aware learning setup, where a latent context is learned over a large range of training tasks. At test time, the learned latent representation is used to infer the new context [22], [10], or optimized for generalization [20], [31], [33]. [20], [31] identify and encode dynamics parameters of a robot into a latent representation and learn a policy conditioned on this latent input. However, these approaches require expert knowledge to determine the dynamics parameters to encode the latent representation, which can be difficult to choose when learning policies across robots of different morphologies. Instead, we propose to automatically learn an embedding space for each robot, obviating the need for expert domain knowledge in defining parameters to encode.

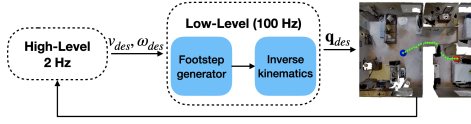


Fig. 3: A flowchart describing our hierarchical control architecture. The high-level controller, described in Section III-B, commands a desired CoM linear and angular velocity. The low-level generates a foot trajectory followed using Inverse Kinematics on the robot.

### III. DYNAMICS-AWARE NAVIGATION POLICIES

In this section, we introduce our approach which learns a dynamics-aware navigation policy that can be applied to previously unseen robots and scenes. We consider hierarchical navigation policies that divide the control of legged robots into a high-level policy that commands desired linear and angular center of mass (CoM) velocities, and a low-level policy which achieves these desired commands (Fig. 3).

#### A. Task: PointGoal Navigation

We consider the task of PointGoal Navigation (PointNav), as defined by [6], in which a robot is initialized in an unseen environment and must navigate to a goal location without the use of a map. An episode is considered successful if the robot can reach within 0.36m of the goal location (approximately half the width of our largest robot) in less than 150 maximum steps, or 120 maximum collisions. In our experiments, the robot is equipped with an egocentric depth sensor and an egomotion estimator (like an IMU) for localization. From the egomotion estimator, the robot has access to the goal coordinates specified relative to the robot at every step. The environments consist of cluttered indoor spaces and the robot has to reason about moving around obstacles to reach a randomly selected goal. For evaluation, we consider the success rate of our policy at reaching random new goals, as well as, Success weighted by (normalized inverse) Path Length (SPL) [6] to measure the efficiency of the path taken.

#### B. Navigation policies with robot-specific embedding

We propose learning a high-level navigation policy that consists of a robot-specific embedding, and a common policy shared across multiple robots. We use soft-actor critic (SAC) with an Autoencoder (AE) [30] as the off-policy training approach of our choice. Unlike, [30], we use egocentric images from the robot’s camera, instead of a global camera. Since the camera is mounted on the robot, the image input changes as the robot moves through the space, for example as the robot base tilts, and the policy has to be robust to such dynamic camera movements. This is not considered by prior navigation literature, which assumes idealized virtual agents.

Apart from training an AE actor and critic, we also aim to learn a robot-specific embedding. We formulate our actor  $\pi_\theta$  to take as input both the observed state  $s$  and a latent embedding  $z_i$  per robot  $i = 1, 2, \dots, N$ , where  $N$  is the total number of robots used during training. The action (desired CoM velocities) is a function of the state and the robot-specific embedding:  $a \sim \pi_\theta(a \mid s, z_i)$ . The critic is formulated similarly, where the predicted Q-value is a function of the state-action pair as well as  $z_i$ :

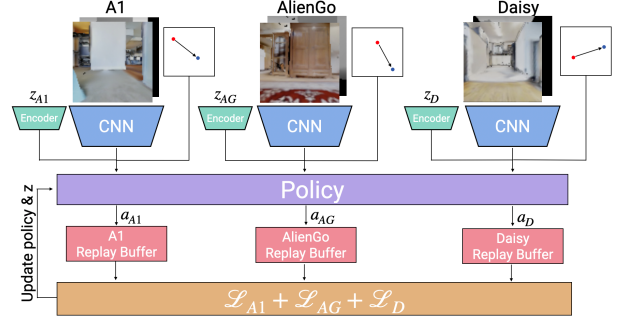


Fig. 4: We train a shared high-level policy for A1, AlienGo, and Daisy jointly. The robots receive an egocentric RGB or Depth observation, the goal relative to the robot’s current position, and a robot-specific embedding. Each robot contributes to a replay buffer, used to calculate total actor and critic loss and update policy.

$Q_\phi(s, a, z_i) = r(s, a) + \bar{V}(s', z_i)$ , where  $Q_\phi$  is the critic,  $r$  is the measured reward and  $\bar{V}(s', z_i)$  is the robot-specific target value function using the max-entropy update rule [14].

Given replay buffers  $\mathcal{D}_i = \{(s, a, s', r, z_i)\}$  from robots  $i = 1 \dots N$ , we create a common collected buffer  $\mathcal{D} = \{\mathcal{D}_1, \mathcal{D}_2, \dots, \mathcal{D}_N\}$ . The soft Bellman residual with robot embeddings becomes a variant of the residual from [14]:

$$\mathcal{L}_{critic} = \mathbb{E}_{(s, a, s', r, z) \sim \mathcal{D}} [Q_\phi(s, a, z) - (r + \bar{V}(s', z))]^2 \quad (1)$$

Both critic parameters  $\phi$  and robot embeddings  $z$  are learned by minimizing  $\mathcal{L}_{critic}$ , assuming  $\bar{V}(s', z)$  to be constant.

$$z_1^*, \dots, z_N^*, \phi^* = \underset{z_1, \dots, z_N, \phi}{\operatorname{argmin}} \mathcal{L}_{critic}(\mathcal{D}) \quad (2)$$

$$\frac{\partial \mathcal{L}_{critic}}{\partial \phi} = \frac{\partial}{\partial \phi} \mathbb{E}_{\mathcal{D}} [Q_\phi(s, a, z) - (r + \gamma \bar{V}(s', z))]^2 \quad (3)$$

$$\frac{\partial \mathcal{L}_{critic}}{\partial z_i} = \frac{\partial}{\partial z_i} \mathbb{E}_{\mathcal{D}_i} [Q_\phi(s, a, z_i) - (r + \gamma \bar{V}(s', z_i))]^2 \quad (4)$$

The partial derivative of  $\mathcal{L}_{critic}$  with respect to  $\phi$  uses samples from all robots, while when updating  $z_i$  the partial derivative w.r.t  $z_{j \neq i}$  is 0. This results in an update law that pools data across multiple robots to update the critic parameters  $\phi$ , but individual robot datasets  $\mathcal{D}_i$  for updating robot-specific embedding  $z_i$ . The actor  $\pi_\theta$  is updated using the common dataset  $\mathcal{D}$ , without updating robot embedding  $z_i$ , by minimizing KL divergence between  $\pi_\theta$  and the predicted optimal Q-value, as in [14]. By collecting data across multiple robots and environments for training both  $\pi_\theta$  and  $Q_\phi$ , our training is more sample-efficient than training per robot, as well as robust to differences in robot dynamics.

We present  $z_i$  as scalar variables for clarity, but they can be generalized to higher-dimensional encoders, whose parameters and inputs are optimized using gradient descent and  $z_i$  becomes the learned, fixed output of the  $z$  encoder. Such learned embeddings have been explored in literature before, for example in [20], [22], [18], [10]. However, none of these works generalize to multiple robot morphologies or use a high-dimensional image input as state. [20], [22], [10] use dynamics randomization to create perturbed environments; [20] input the dynamics parameters to learn the embedding, while [22], [10] use robot state trajectories of



past time steps as input. In contrast, we present a fully-learned embedding which does not need hand-defined inputs, and can automatically learn an embedding for significantly different robot morphologies. We also compare our approach against [20] and [10], and show that we outperform both.

### C. Generalization to unseen robots

Once the actor, critic and robot embeddings are trained, we can adapt our learned navigation policies to new robots by directly searching in the space of learned embeddings. We aim to find a robot embedding  $z_{test}^*$  that maximizes the long-term reward over trajectories  $\tau$  of length  $T$  induced on the test platform, using the learned policy  $\pi_\theta(\cdot, z_{test}^*)$ .

$$z_{test}^* = \underset{z_{test}}{\operatorname{argmax}} \mathbb{E}_\tau \left[ \sum_{t=1}^T r_t \right] \quad (5)$$

We conduct a grid-search over  $z_{test}$  to find the globally-optimal  $z_{test}^*$  (within discretization error) in the space of learned embeddings. Approximate techniques like [20], [32] can be used for higher dimensional  $z$ .

For successful navigation on new robots, the learned embedding should capture different properties that different robots demonstrate. For example, some robots might be slower at turning while others might be faster. We expect different samples of  $z$  to result in different desired motions of robots around obstacles, etc. Fig. 5 illustrates different samples in the latent space and corresponding high-level center of mass (CoM) trajectories in an environment with obstacles. With  $z = -0.7$ , we see that 4-legged Daisy takes a relatively direct path to the goal, while with other  $z$  values, the robot makes larger turns and gets stuck on obstacles.

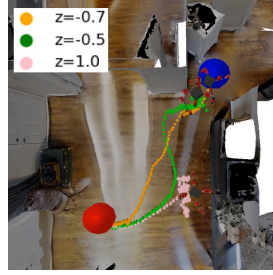


Fig. 5: Modulating the policy with different  $z_{test}$  results in different CoM trajectories followed by 4-legged Daisy.

### D. Low-level controllers for legged robots

Our low-level policy shares a common structure across robots by converting desired CoM velocities into desired footstep locations. The footsteps are then followed using robot-specific kinematics information.

Each low-level step consists of one physical robot step taking  $\Delta t = 0.5s$ , consisting of  $N_{step} = 50$  simulation steps. During this robot step, the robot's foot moves from current location  $(x_{cur}^f, y_{cur}^f)$ , relative to the CoM, to a desired foot placement location  $(x_{des}^f, y_{des}^f)$ . Given desired CoM linear velocity  $v_{des}$  and angular velocity  $\omega_{des}$  from the high-level, an expert-designed feedback policy calculates the desired change in footstep position  $(\delta x^f, \delta y^f)$  using the desired change in CoM position  $\delta x_{com} = v_{des} \Delta t$  and orientation  $\delta \gamma_{com} = \omega_{des} \Delta t$ . For turning, the foot moves in a circle of radius  $r$ , changing the current angle between the foot and the robot heading  $\gamma_{cur}^f$  to  $\gamma_{des}^f = \gamma_{cur}^f + \delta \gamma_{com}$  at the end of

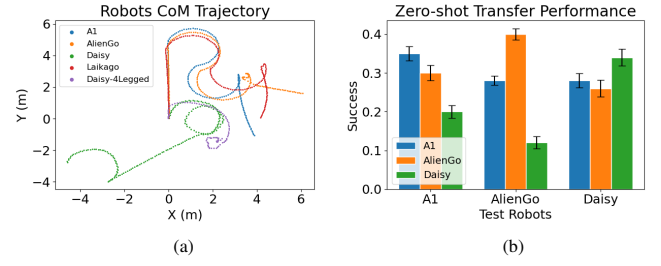


Fig. 6: (a): Center of Mass (CoM) trajectories for different robots following the same high-level commands. Due to the differences in the low-level controller, each robot ends up taking a different trajectory, with A1, AlienGo, Laikago very different from Daisy and 4-legged Daisy. (b) Zero-shot transfer of policies trained on a single robot onto other robots. Each robot performs best with a policy trained on itself, and performance deteriorates when using a policy trained on a different robot.

the step.

$$\delta x_f = \delta x_{com} + r \cdot (\cos(\gamma_{des}^f) - \cos(\gamma_{cur}^f)) \quad (6)$$

$$\delta y_f = r \cdot (\sin(\gamma_{des}^f) - \sin(\gamma_{cur}^f)) \quad (7)$$

$$x_{f,des} = x_{f,cur} + \delta x_f \quad y_{f,des} = y_{f,cur} + \delta y_f \quad (8)$$

where  $r = \sqrt{(x_{cur}^f)^2 + (y_{cur}^f)^2}$  is the distance between the foot and CoM, and  $\gamma_{curr}^f = \arctan(y_{cur}^f/x_{cur}^f)$  is the relative angle between robot heading and robot foot. Such a hierarchical architecture for control is very common in legged robots and many heuristics exist in literature for calculating footstep location based on desired CoM motion, for example using simple models like inverted pendulums [12] or spring mass models [28], [19]. Our policy is inspired from [21] and [16], with an added orientation for 3D motion. Stance joint trajectories are designed to mirror the swing joint trajectories, as in [21].

Our footstep planner can be applied to a large range of legged robots, such as hexapods and quadrupeds. This enables us to use the same low-level policy structure to experiment with 5 different legged robot designs, which is usually cumbersome due to robot-specific low-level policies. As our low-level policy is shared across multiple robots, it is not perfect at following the high-level commands for all robots. The performance and stability of the low-level policy could potentially be improved by tuning the policy for each robot, at the cost of bringing down the scalability of our approach. Fig. 6a shows the CoM trajectories that different robots exhibit given the same high-level action sequence using our low-level controller. While A1, AlienGo and Laikago have similar trajectories in the start, they diverge later. On the other hand, Daisy and 4-legged Daisy have significantly different trajectories, and tend to turn to the left using our low-level controller. Fig. 6b shows the accumulative performance of pairing different low-level controllers of each robot with high-level policies trained on other robots. Each robot performs best when using a high-level policy that was trained with its own controller, and performance deteriorates when using high-level policies trained on other robots, with AlienGo performance going down from  $0.40 \pm 0.10$  to  $0.26 \pm 0.15$  when using its own policy, vs. Daisy

policy. These results empirically confirm our hypothesis that each legged robot has sufficiently different dynamics that need to be accounted for by the high-level policy in order to achieve good navigation performance, even when the low-level controllers share a common structure.

Learning a shared high-level policy also allows robots to share data, significantly improving the sample-efficiency of learning. Our hierarchical controller makes training of the high-level policy even more expensive than usual. For every action commanded by the high-level policy, the low-level policy takes  $N_{step}$  simulation steps to achieve the desired command. Hence, the number of the data points collected per high-level action is  $\frac{1}{N_{step}}$  of the actual simulation steps. By pooling data across  $N$  robots, we effectively get  $N$  times as much data as we would if we collected data per robot. Our experiments show that our hierarchical structure with off-policy high-level learning can learn navigation policies for multiple legged robots in a small number of samples, and generalize to unseen robots.

#### IV. EXPERIMENTAL EVALUATION

We evaluate our proposed approach on two experimental setups - a set of cart-pole variants, and a set of legged robots. In both cases, we aim to learn generalizable policies on certain morphologies and test on new morphologies that were not seen during training. We first choose cart-pole environments as a simplified, but illustrative example of our framework, and compare with other approaches from literature. Our results show that our approach is faster at learning on a set of cart-poles, and better at generalization to unseen cart-poles than other approaches, like [10], [20]. Next, we tackle the much more challenging task of learning navigation policies on legged robots, and generalization to unseen robots. Our experiments show that our hierarchical controllers can learn navigation policies across multiple legged robots, and generalize to unseen robots sample-efficiently, outperforming oracle point-agent policies. We train all approaches on 3 train robots, and evaluate generalization to 2 new robots.

##### A. Experimental setup

We compare our approach (**Learned-z**) to the following baselines and ablations of our approach:

- **RL<sup>2</sup> with DDPG (Meta-RL)**: We use RL<sup>2</sup> [10] as a baseline that learns robot-specific contexts during training. At test time, context is inferred from state trajectories on the test robot. This baseline compares our learned robot-specific embedding to meta-learned embeddings from literature.

- **Informed embedding (Informed-z)**: [20] learn a robot-specific embedding by giving dynamics parameters of robots as input to the  $z$  encoder. At test time,  $z$  is optimized for new robot, same as our approach. This experiment compares our learned embedding, which does not require any prior knowledge of the dynamics parameters, to an informed embedding that has access to more privileged information.

- **Semi-Informed embedding (Semi-Informed-z)**: In this experiment, we only give a sub-set of the varied dynamics parameters as inputs to the  $z$  encoder during training (mass

and offset of the cart-poles). Deciding the ‘right’ input parameters can be challenging, especially when working with different robot morphologies. This experiment shows the sensitivity of [20] to incorrect set of parameters.

- **Fixed robot embedding (Fixed-z)**: In this ablation of our approach, we use a randomly-chosen fixed  $z$  for train environments. At test time,  $z$  is optimized for new robot, same as our approach. This experiment demonstrates that a learned embedding captures the landscape of robot dynamics better than randomly initialized embeddings.

- **No robot-specific embedding (No-z)**: In this ablation of our approach, we learn a shared policy across different environments, with no robot-specific embeddings. At test time, the whole policy is fine-tuned on the new robot. This experiment demonstrates the need for embeddings for sample-efficient generalization.

##### B. Cart-pole experiments

We create a family of cart-poles in Mujoco [26] by changing the mass of cart, length of pole, and offset of pole from center (Fig. 7, Table I). Test robots consist of one cart-pole that lies ‘between’ the training cart-poles (CP5) and one that lies outside of the training distribution (CP4). Our aim is to test generalization of all approaches to both in and out-of-distribution robots. We visualize the learned latent space using our approach on all cart-poles by sweeping over different values of  $z$  and measuring performance (Fig. 7, bottom). Except CP1, all train cart-poles have a singular maximum, near the learned  $z$ . Visualizing the latent space also shows that CP4 is close to CP3 in learned latent space, but out of distribution from train robots, while CP5 is between CP2 and CP3, as expected. This demonstrates that the learned embedding has captured dynamics properties of the robots, and is capable of interpolating and extrapolating over train robot dynamics.

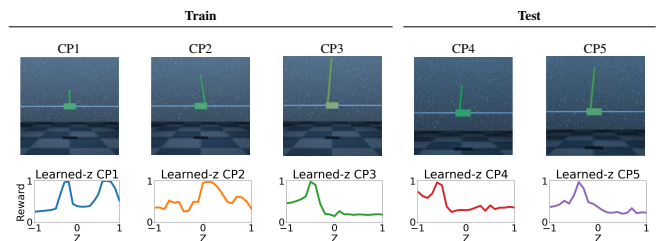


Fig. 7: (Top) Cart-pole robots used for training and testing. (Bottom) Performance of cart-poles for different  $z$  in the learned latent space.

TABLE I: We create 5 variants of cart-poles with dynamics parameters shown below. We train on CP1-3, and test on CP4,5.

Parameter	Train			Test	
	CP1	CP2	CP3	CP4	CP5
Mass	0.1	1	2	1.5	1.5
Pole Length	0.5	1	1.5	0.75	1.25
Pole Offset	0	0.15	-0.15	-0.1	-0.1

The results of our cart-pole experiments on CP3 are shown in Fig. 8, and Table II condenses results for all cart-poles.

TABLE II: Cart-pole Evaluation Performance

Experiment	Train			Test	
	CP1 Ep. Reward	CP2 Ep. Reward	CP3 Ep. Reward	CP4 Ep. Reward	CP5 Ep. Reward
Semi-Informed-z	0.97 $\pm$ 0.02	0.74 $\pm$ 0.03	0.71 $\pm$ 0.04	0.42 $\pm$ 0.04	0.75 $\pm$ 0.01
Meta-RL <sub>3envs</sub>	0.99 $\pm$ 0.01	0.93 $\pm$ 0.02	0.70 $\pm$ 0.09	0.66 $\pm$ 0.11	0.83 $\pm$ 0.06
Meta-RL <sub>5envs</sub>	<b>1.00<math>\pm</math>0.01</b>	0.91 $\pm$ 0.01	0.91 $\pm$ 0.04	0.89 $\pm$ 0.04	0.93 $\pm$ 0.03
Informed-z	0.99 $\pm$ 0.01	0.90 $\pm$ 0.04	0.93 $\pm$ 0.02	0.79 $\pm$ 0.16	0.94 $\pm$ 0.04
No-z	0.99 $\pm$ 0.01	0.76 $\pm$ 0.08	0.80 $\pm$ 0.05	0.68 $\pm$ 0.10	0.85 $\pm$ 0.06
Fixed-z	0.99 $\pm$ 0.02	0.86 $\pm$ 0.13	0.87 $\pm$ 0.19	0.77 $\pm$ 0.21	<b>0.97<math>\pm</math>0.03</b>
Learned-z	<b>1.00<math>\pm</math>0.00</b>	<b>0.98<math>\pm</math>0.00</b>	<b>0.98<math>\pm</math>0.01</b>	<b>0.94<math>\pm</math>0.03</b>	<b>0.97<math>\pm</math>0.03</b>

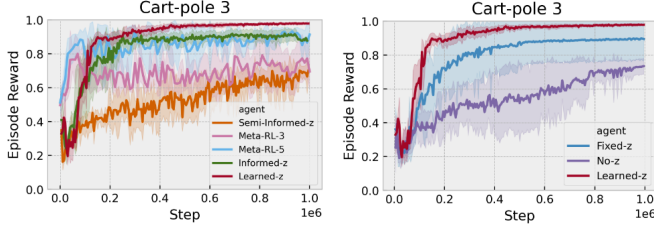


Fig. 8: Learning speed of different approaches, visualized on CP3. Our approach learns faster, and achieves a higher performance than all the other approaches. (Left) Comparison against context-aware approaches; (Right) Ablations of our approach.

We consider two variants of RL<sup>2</sup> – **Meta-RL<sub>3envs</sub>** and **Meta-RL<sub>5envs</sub>**. **Meta-RL<sub>3envs</sub>** sees only 3 of the 5 cart-poles during training, and is tested on the 2 held-out cart-poles. **Meta-RL<sub>5envs</sub>** sees all 5 cart-poles during training and is tested on one of the training cart-poles. **Meta-RL<sub>3envs</sub>** does not learn to control CP3, and performs poorly on test cart-poles CP4 and CP5 (0.66 $\pm$ 0.11 on CP4 and 0.83 $\pm$ 0.06 on CP5), showing that **Meta-RL<sub>3envs</sub>** is unable to generalize to new unseen robots. As can be expected, the performance of **Meta-RL<sub>5envs</sub>** is better than **Meta-RL<sub>3envs</sub>**, as the learned embedding is trained on all cart-poles, requiring just inference of test cart-pole, and no generalization.

**Meta-RL<sub>5envs</sub>**, **Informed-z** and **Learned-z** learn at a similar rate, but **Learned-z** generalizes to test robot CP4 better (0.94 $\pm$ 0.03 using **Learned-z** vs 0.79 $\pm$ 0.16 using **Informed-z** and 0.89 $\pm$ 0.04 using **Meta-RL<sub>5envs</sub>**). This indicates that for **Informed-z**, the additional information of dynamics parameters deteriorates generalization to out-of-distribution robots. **Semi-Informed-z** performs poorly at training and generalization experiments, highlighting the sensitivity of [20] to the ‘right’ set of dynamics parameters. Among the ablation experiments of our approach, **Learned-z**, **No-z** and **Fixed-z**, we observe that **Learned-z** generalizes better to the two test robots. While both **Learned-z** and **Fixed-z** learn to control the training cart-poles, generalization to CP4 is improved when using learned robot embeddings (0.94 $\pm$ 0.03 with **Learned-z** vs 0.77 $\pm$ 0.21 with **Fixed-z** and 0.68 $\pm$ 0.1 with **No-z**). **Meta-RL<sub>5envs</sub>**, **Informed-z** and **Fixed-z** are close to **Learned-z** in generalization to in-distribution test robot (CP5), but **Learned-z** performs best when testing on out-of-distribution robot (CP4).

### C. Legged robot experiments

Next, we present experiments on legged robots (Fig. 9). In this setting, we use the hierarchical control structure

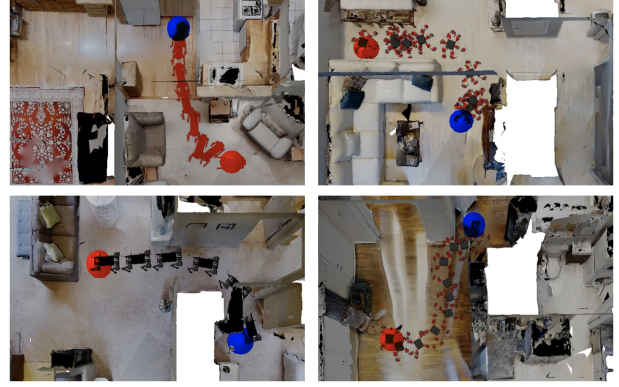


Fig. 9: Learned navigation policies on different train (top; AlienGo and Daisy) and test (bottom; Laikago and 4-legged Daisy) robots.

described in Section III-D as the controller. Robots are trained from scratch for cumulative 1 million simulation steps across all robots on a single GPU.

Row 1 in Table III shows the performance of navigation policies trained without knowledge of the robot’s dynamics applied to legged robots. We consider an oracle point-based policy which uses a map of the environment find a near-optimal collision-free path to goal. An idealized agent is able to achieve near perfect performance using the path produced by the oracle (0.92 $\pm$ 0.04 SPL). When applied on the legged robots, the performance drops significantly, with the most significant drop seen on 4-legged Daisy (0.18 $\pm$ 0.06 SPL). This is because the oracle policy does not account for robot dynamics, and the robots often fall, get stuck around an obstacle, or do not reach the goal in maximum allowed steps. This result emphasizes that incorporating the low-level dynamics of legged robots is crucial for effective navigation of cluttered spaces.

We do not compare against **Informed-z**, and **Meta-RL** on legged robots as defining the right set of input parameters or states is non-trivial for legged robots with different morphologies. Among the ablations of our approach, we observe similar performance between **Learned-z** and **Fixed-z** at learning to control the training robots, slightly outperforming **No-z**. However, on generalization robots we see an improvement when using **Learned-z** especially on 4-legged Daisy (0.49 $\pm$ 0.08 with **Learned-z** vs 0.38 $\pm$ 0.11 with **Fixed-z** and 0.22 $\pm$ 0.08 with **No-z**). Since 4-legged Daisy is the most ‘different’ robot from the train robots, we again observe that our approach performs better at out-of-distribution generalization.

TABLE III: Legged Robots’ Evaluation Performance

Experiment	Train			Test		
	A1 SPL	AlienGo SPL	Daisy SPL	Laikago SPL	Daisy4 SPL	Sphere SPL
No-dynamics	0.49 $\pm$ 0.07	0.45 $\pm$ 0.15	0.22 $\pm$ 0.10	0.38 $\pm$ 0.15	0.18 $\pm$ 0.06	0.92 $\pm$ 0.04
No-z	0.48 $\pm$ 0.12	0.42 $\pm$ 0.05	0.33 $\pm$ 0.07	0.33 $\pm$ 0.13	0.22 $\pm$ 0.08	-
Fixed-z	<b>0.59<math>\pm</math>0.07</b>	<b>0.59<math>\pm</math>0.14</b>	0.40 $\pm$ 0.10	0.47 $\pm$ 0.09	0.38 $\pm$ 0.11	-
Learned-z	<b>0.59<math>\pm</math>0.07</b>	0.54 $\pm$ 0.04	<b>0.48<math>\pm</math>0.14</b>	<b>0.48<math>\pm</math>0.08</b>	<b>0.49<math>\pm</math>0.08</b>	-

## V. CONCLUSION

In this work, we present a framework for learning hierarchical navigation policies for legged robots. Our policy shares data across multiple robots during learning, and learns

a shared navigation policy with robot-specific embeddings, which are used for specialization. The learned embedding captures different dynamical properties, such as turning radius and walking speed of different robots, and shows promising results even on robots that were never seen during training. We demonstrate our approach can sample-efficiently generalize to new legged robots at test time and is robust to dynamic differences between robots. This work opens up future avenues for large-scale research on legged platforms for indoor navigation.

## VI. ACKNOWLEDGEMENTS

The Georgia Tech effort was supported in part by NSF, AFRL, DARPA, ONR YIPs, ARO PECASE. JT was supported by an NSF Graduate Research Fellowship under Grant No. DGE-1650044 and a Google Women Techmaker's Fellowship. The views and conclusions are those of the authors and should not be interpreted as representing the U.S. Government, or any sponsor.

**License for dataset used** Gibson Database of Spaces. License at [http://svl.stanford.edu/gibson2/assets/GDS\\_agreement.pdf](http://svl.stanford.edu/gibson2/assets/GDS_agreement.pdf)

## REFERENCES

- [1] Boston dynamics. <https://www.bostondynamics.com/spot>. Accessed: 2020-10-10.
- [2] Ghost robotics. <https://www.ghostrobotics.io/>. Accessed: 2020-10-10.
- [3] Hebi robotics. <https://www.hebirobotics.com/robotic-kits>.
- [4] Sim2real challenge with igibson. <http://svl.stanford.edu/igibson/challenge.html>. Accessed: 2020-10-10.
- [5] Unitree robotics. <https://www.unitree.com/>. Accessed: 2020-10-10.
- [6] Peter Anderson, Angel Chang, Devendra Singh Chaplot, Alexey Dosovitskiy, Saurabh Gupta, Vladlen Koltun, Jana Kosecka, Jitendra Malik, Roozbeh Mottaghi, Manolis Savva, et al. On Evaluation of Embodied Navigation Agents. *arXiv preprint arXiv:1807.06757*, 2018.
- [7] Somil Bansal, Varun Tolani, Saurabh Gupta, Jitendra Malik, and Claire Tomlin. Combining optimal control and learning for visual navigation in novel environments. In *Conference on Robot Learning*, pages 420–429. PMLR, 2020.
- [8] Sean L Bowman, Nikolay Atanasov, Kostas Daniilidis, and George J Pappas. Probabilistic data association for semantic slam. In *2017 IEEE international conference on robotics and automation (ICRA)*, pages 1722–1729. IEEE, 2017.
- [9] Erwin Coumans and Yunfei Bai. Pybullet, a python module for physics simulation for games, robotics and machine learning. <http://pybullet.org>, 2016–2019.
- [10] Yan Duan, John Schulman, Xi Chen, Peter L Bartlett, Ilya Sutskever, and Pieter Abbeel. RL<sup>2</sup>: Fast reinforcement learning via slow reinforcement learning. *arXiv preprint arXiv:1611.02779*, 2016.
- [11] Hugh Durrant-Whyte and Tim Bailey. Simultaneous localization and mapping: part i. *IEEE robotics & automation magazine*, 13(2):99–110, 2006.
- [12] Siyuan Feng, Eric Whitman, X Xinjilefu, and Christopher G Atkeson. Optimization-based full body control for the darpa robotics challenge. *Journal of Field Robotics*, 32(2):293–312, 2015.
- [13] Jorge Fuentes-Pacheco, José Ruiz-Ascencio, and Juan Manuel Rendón-Mancha. Visual simultaneous localization and mapping: a survey. *Artificial intelligence review*, 43(1):55–81, 2015.
- [14] Tuomas Haarnoja, Aurick Zhou, Kristian Hartikainen, George Tucker, Sehoon Ha, Jie Tan, Vikash Kumar, Henry Zhu, Abhishek Gupta, Pieter Abbeel, et al. Soft actor-critic algorithms and applications. *arXiv preprint arXiv:1812.05905*, 2018.
- [15] Wolfgang Hess, Damon Kohler, Holger Rapp, and Daniel Andor. Real-time loop closure in 2d lidar slam. In *2016 IEEE International Conference on Robotics and Automation (ICRA)*, pages 1271–1278. IEEE, 2016.
- [16] Christian Hubicki, Andy Abate, Patrick Clary, Siavash Rezazadeh, Mikhail Jones, Andrew Peekema, Johnathan Van Why, Ryan Domres, Albert Wu, William Martin, et al. Walking and running with passive compliance: Lessons from engineering: A live demonstration of the atrias biped. *IEEE Robotics & Automation Magazine*, 25(3):23–39, 2018.
- [17] Abhishek Kadian, Joanne Truong, Aaron Gokaslan, Alexander Clegg, Erik Wijmans, Stefan Lee, Manolis Savva, Sonia Chernova, and Dhruv Batra. Sim2real Predictivity: Does Evaluation in Simulation Predict Real-World Performance? *IEEE Robotics and Automation Letters*, 2020.
- [18] Tianyu Li, Roberto Calandra, Deepak Pathak, Yuandong Tian, Franziska Meier, and Akshara Rai. Planning in learned latent action spaces for generalizable legged locomotion. *arXiv preprint arXiv:2008.11867*, 2020.
- [19] William C Martin, Albert Wu, and Hartmut Geyer. Experimental evaluation of deadbeat running on the atrias biped. *IEEE Robotics and Automation Letters*, 2(2):1085–1092, 2017.
- [20] Xue Bin Peng, Erwin Coumans, Tingnan Zhang, Tsang-Wei Lee, Jie Tan, and Sergey Levine. Learning agile robotic locomotion skills by imitating animals. *arXiv preprint arXiv:2004.00784*, 2020.
- [21] Marc H Raibert. *Legged robots that balance*. MIT press, 1986.
- [22] Kate Rakelly, Aurick Zhou, Chelsea Finn, Sergey Levine, and Deirdre Quillen. Efficient off-policy meta-reinforcement learning via probabilistic context variables. In *International conference on machine learning*, pages 5331–5340, 2019.
- [23] Fereshteh Sadeghi and Sergey Levine. Cad2rl: Real single-image flight without a single real image. *arXiv preprint arXiv:1611.04201*, 2016.
- [24] Manolis Savva, Abhishek Kadian, Oleksandr Maksymets, Yili Zhao, Erik Wijmans, Bhavana Jain, Julian Straub, Jia Liu, Vladlen Koltun, Jitendra Malik, Devi Parikh, and Dhruv Batra. Habitat: A Platform for Embodied AI Research. In *ICCV*, 2019.
- [25] Sebastian Thrun. Probabilistic robotics. *Communications of the ACM*, 45(3):52–57, 2002.
- [26] E. Todorov, T. Erez, and Y. Tassa. Mujoco: A physics engine for model-based control. *2012 IEEE/RSJ International Conference on Intelligent Robots and Systems*, pages 5026–5033, 2012.
- [27] Erik Wijmans, Abhishek Kadian, Ari Morcos, Stefan Lee, Irfan Essa, Devi Parikh, Manolis Savva, and Dhruv Batra. Dd-ppo: Learning near-perfect pointgoal navigators from 2.5 billion frames. *arXiv*, pages arXiv–1911, 2019.
- [28] Albert Wu and Hartmut Geyer. The 3-d spring-mass model reveals a time-based deadbeat control for highly robust running and steering in uncertain environments. *IEEE Transactions on Robotics*, 29(5):1114–1124, 2013.
- [29] Fei Xia, William B Shen, Chengshu Li, Priya Kasimbeg, Micael Edmond Tchammi, Alexander Toshev, Roberto Martín-Martín, and Silvio Savarese. Interactive gibbon benchmark: A benchmark for interactive navigation in cluttered environments. *IEEE Robotics and Automation Letters*, 5(2):713–720, 2020.
- [30] Denis Yarats, Amy Zhang, Ilya Kostrikov, Brandon Amos, Joelle Pineau, and Rob Fergus. Improving sample efficiency in model-free reinforcement learning from images. 2019.
- [31] Wenhao Yu, Visak CV Kumar, Greg Turk, and C Karen Liu. Sim-to-real Transfer for Biped Locomotion. *arXiv preprint arXiv:1903.01390*, 2019.
- [32] Wenhao Yu, Jie Tan, Yunfei Bai, Erwin Coumans, and Sehoon Ha. Learning fast adaptation with meta strategy optimization. *IEEE Robotics and Automation Letters*, 5(2):2950–2957, 2020.
- [33] Wenhao Yu, Jie Tan, C Karen Liu, and Greg Turk. Preparing for the unknown: Learning a universal policy with online system identification. *arXiv preprint arXiv:1702.02453*, 2017.